

Modern nuclear force predictions for the neutron-deuteron scattering lengths

H. Witała^{1,2}, A. Nogga³, H. Kamada⁴, W. Glöckle⁵, J. Golak¹, R. Skibiński¹.

¹*M. Smoluchowski Institute of Physics, Jagiellonian University, PL-30059 Kraków, Poland*

²*Department für Physik und Astronomie, Universität Basel, Basel, Switzerland*

³*Department of Physics, University of Arizona, Tucson, Arizona 85721*

⁴*Department of Physics, Faculty of Engineering, Kyushu Institute of Technology, 1-1 Sensuicho, Tobata, Kitakyushu 804-8550, Japan*

⁵*Institut für Theoretische Physik II, Ruhr-Universität Bochum, D-44780 Bochum, Germany*
(August 21, 2018)

Abstract

The neutron-deuteron (nd) doublet (${}^2a_{nd}$) and quartet (${}^4a_{nd}$) scattering lengths have been calculated based on the nucleon-nucleon (NN) interactions CD Bonn 2000, AV18, Nijm I, II and 93 alone and in selected combinations with the Tucson-Melbourne (TM), a modified version thereof, TM99, and the Urbana IX three-nucleon (3N) forces. For each NN and 3N force combination also the 3H binding energy was calculated. In case of TM99 and Urbana IX the 3NF parameters were adjusted to the 3H binding energy. In no case (using np-nn forces) the experimental value of ${}^2a_{nd}$ was reached. We also studied the effect of the electromagnetic interactions in the form introduced in AV18. Switching them off for the various nuclear force models leads to shifts of up to +0.04 fm for ${}^2a_{nd}$, which is significant for present day standards. The electromagnetic effects have also a noticeable effect on ${}^4a_{nd}$, which otherwise is extremely stable under the exchange of the nuclear forces. Only when the electromagnetic interactions are included the current nuclear forces describe the experimental value. As a consequence of the failure to reproduce ${}^2a_{nd}$ also the newly measured coherent nd scattering length (b_{nd}) can not be reproduced. For the current nuclear force models there is a strong scatter of the 3H binding energy and the ${}^2a_{nd}$ values around an averaged straight line (Phillips line). This allows to use ${}^2a_{nd}$ and the 3H binding energy as independent low energy observables.

21.45.+v, 24.70.+s, 25.10.+s, 25.40.Lw

I. INTRODUCTION

It has been observed a long time ago that the nd scattering length for total three-nucleon spin $S=1/2$ (${}^2a_{nd}$) is correlated to the 3H binding energy (E_{3H}). This correlation is known as the Phillips line [1]. Indeed, calculations years later based on simplistic or more realistic NN model forces (see [2–7]) yielded quite a few results for the 3H binding energy and the ${}^2a_{nd}$ scattering length, which lie on or rather close to a line in the two-dimensional plane spanned by E_{3H} and ${}^2a_{nd}$. Also 3N forces of the 2π -exchange type have been added. In [3] it was found that this line passes well through the experimental point.

In recent years chiral perturbation theory and effective theories have been applied to nuclear physics. In the pionless formulation [8–10], adequate for extreme low energy phenomena, it has been shown that 3H can be energetically stabilized only if a 3N contact force is introduced (see however [11,12]). In the two lowest orders of that framework there is just one parameter connected to that 3N force. Thus both quantities, E_{3H} and ${}^2a_{nd}$, depend on that one parameter and are therefore correlated though the line does not hit the experimental point. In higher orders additional parameters show up and the correlation is broken, which makes the two quantities independent. The same observation was made in an approach based on chiral perturbation theory [13] which includes explicitly the pion degrees of freedom. In the next-to-next-to-leading-order (NNLO), 3N forces occur the first time and they depend on two parameters. This makes E_{3H} and ${}^2a_{nd}$ independent and the Phillips line correlation is broken. In fact in that framework the two experimental values are used to fix those two parameters of the 3N force [13]. Thus we find it interesting to ask, whether the conventional and high precision NN forces AV18 [14], CD Bonn 2000 [15], Nijm I, Nijm II, and Nijm 93 [16] alone or in combination with the two most popular 3N force models, Urbana IX [17] and TM99 [18,19] (an updated Tucson-Melbourne 2π -exchange 3NF [20] modified in view of chiral symmetry) lead to a strict correlation between E_{3H} and ${}^2a_{nd}$ or whether that Phillips line correlation is also broken. Further we ask whether the NN and 3NF combinations adjusted to E_{3H} (or may be only one of them) also describe ${}^2a_{nd}$. One more reason to confront ${}^2a_{nd}$ to state-of-the-art calculations is the recent appearance of a precision neutron interferometric measurements of the nd coherent scattering length (b_{nd}) [21].

The coherent scattering length b_{nd} depends in addition to ${}^2a_{nd}$ also on the second s-wave scattering length for the state of total 3N spin $S=3/2$, ${}^4a_{nd}$. Because of the Pauli principle this quantity is supposed not to be sensitive to short range details of nuclear forces. We want to investigate also that quantity in the light of modern nuclear forces.

Then we would like to add two more investigations. Charge-symmetry breaking (CSB) in the strong NN forces is mostly pronounced in the states 1S_0 , where the scattering length for the neutron-neutron (nn), a_{nn} , and proton-proton (pp), a_{pp} , systems are different. However the value for a_{nn} is still under debate [22,23]. Therefore we would like to present results, where the nn forces are replaced by the (strong) pp forces. This will provide some insight into the magnitudes of the shifts in ${}^2a_{nd}$ caused by small changes in a_{nn} .

The other investigation is due to effects on the scattering lengths and E_{3H} caused by electromagnetic interactions, mostly due to magnetic moment interactions (MMI). MMI is a relativistic effect and including only that specific force is of course inconsistent, since other relativistic effects are not taken into account (see for instance [24] and references therein).

But it is interesting to see its separate effect on ${}^2a_{nd}$ and ${}^4a_{nd}$ (its effect on the binding energy of 3H and 3He is known and older results have been reconfirmed recently [25]). Here we hit some "defects" in current NN force models. The NN potentials CD Bonn 2000, Nijm I, II, and Nijm 93 are fitted directly to the NN data without taking electromagnetic interactions (EMI) into account (of course the point Coulomb force in case of the pp system has been included). Therefore those strong forces include the effects of the MMI's (and further electromagnetic corrections). If we want to see then the separate effects of the EMI's we have to subtract from those model NN forces the EMI's and compare to results without that subtraction. In case of AV18 the strong force plus EMI's have been fitted to the data. Thus the force free of EMI's is just the strong AV18 force alone. In this manner by comparing results with and without electromagnetic interactions one can see their effects.

The paper is organised as follows. In Section II the theoretical formulation is briefly outlined. The results are given in Section III, and we end with a summary and an outlook in Section IV. More technical details are deferred to an appendix.

II. FORMULATION

We use the Faddeev scheme. Including a three-nucleon force a convenient basic formulation for part of the $nd \rightarrow n + n + p$ break-up amplitude T [26,27] is the integral equation

$$T = tP\phi + (1 + tG_0)V_4^{(1)}(1 + P)\phi + tPG_0T + (1 + tG_0)V_4^{(1)}(1 + P)G_0T. \quad (1)$$

The driving term contains the NN t -operator t , permutation operators P , the free 3N propagator G_0 and part of the 3N force, $V_4^{(1)}$. Any 3N force can be split into three pieces, where for instance the first piece is symmetrical under exchange of particles 2 and 3, the second under 3-1 exchange etc. Thus the quantity $V_4^{(1)}$ is the part symmetrical under 2-3 exchange like the t -operator t , which is supposed to act on the pair 23. Finally, ϕ is the initial channel state composed of the deuteron state and a momentum eigenstate of the projectile neutron. That integral equation can be solved precisely in a partial wave decomposition in momentum space. For details see [28,26,29].

The operator U for elastic scattering is given in terms of the amplitude T by quadrature as follows

$$U = PG_0^{-1}\phi + PT + V_4^{(1)}(1 + P)\phi + V_4^{(1)}(1 + P)G_0T. \quad (2)$$

We want to solve the integral equation (1) directly at the threshold of nd scattering. This is for zero initial relative momentum \vec{q}_0 of the projectile and will then lead directly to the scattering length. For the convenience of the reader we briefly sketch the necessary steps [30]. Our partial wave momentum space basis is denoted by $|pq\alpha\rangle$, where p and q are the magnitudes of standard Jacobi momenta and α a string of angular momentum and isospin quantum numbers (see [26,28]). Then for \vec{q}_0 in z -direction we define the auxiliary amplitude

$$U_{\alpha,\lambda I}(p, q) = \sum_{m, m_d} \frac{\sqrt{4\pi\hat{\lambda}}}{\hat{j}} (\lambda 0 \frac{1}{2} m | I m) (j_d m_d I m | J m_d + m) \langle pq\alpha | U | \phi \rangle \quad (3)$$

for the projectile nucleon with orbital angular momentum λ ($\hat{\lambda} \equiv 2\lambda + 1$) and total angular momentum I combined with the deuteron total angular momentum $j_d = 1$ to total 3N angular momentum J . Out of that amplitude one obtains the partial wave projected nd elastic scattering amplitude

$$U_{\lambda'I',\lambda I}^J = \sum_{\nu'} \int p'^2 dp' \phi_{\nu'}(p') U_{\alpha_d, \lambda I}(p', q_0). \quad (4)$$

where $\phi_l(p)$ are the s- and d-wave components of the deuteron and α_d contains the deuteron quantum numbers.

Finally, the projectile spin and the deuteron spin can be combined to the total spin Σ and one obtains

$$U_{\lambda'\Sigma',\lambda\Sigma}^J = \sum_{I,I'} \sqrt{\hat{\Sigma}'\hat{I}'(-)^{J-I'}} \left\{ \begin{matrix} \lambda' & \frac{1}{2} & I' \\ j_d & J & \Sigma' \end{matrix} \right\} \sqrt{\hat{\Sigma}\hat{I}(-)^{J-I}} \left\{ \begin{matrix} \lambda & \frac{1}{2} & I \\ j_d & J & \Sigma \end{matrix} \right\} U_{\lambda'I',\lambda I}^J. \quad (5)$$

The S - matrix element is then given as

$$S_{\lambda'\Sigma',\lambda\Sigma}^J = \delta_{\lambda'\lambda} \delta_{\Sigma'\Sigma} - i \frac{4\pi}{3} m q_0 (i)^{\lambda'-\lambda} U_{\lambda'\Sigma',\lambda\Sigma}^J \quad (6)$$

leading to the doublet and quartet scattering lengths for $q_0 = 0$

$$\begin{aligned} {}^2a_{nd} &= \frac{2\pi}{3} m U_{0\frac{1}{2},0\frac{1}{2}}^{\frac{1}{2}} \\ {}^4a_{nd} &= \frac{2\pi}{3} m U_{0\frac{3}{2},0\frac{3}{2}}^{\frac{3}{2}}. \end{aligned} \quad (7)$$

One also defines a coherent scattering length b_{nd} as

$$b_{nd} = \frac{m_n + m_d}{m_d} \left[\left(\frac{1}{3}\right) {}^2a_{nd} + \left(\frac{2}{3}\right) {}^4a_{nd} \right] \quad (8)$$

We defer the special form of the Faddeev integral equation (1) at $q_0 = 0$ to the appendix. It is free of singularities and therefore as easily solved as a bound state problem. Also the explicit form of the elastic amplitude for $q_0 = 0$ is given there.

III. RESULTS

We used the NN forces CD Bonn 2000, AV18, Nijm I, II and Nijm 93 alone or various combinations with the three-nucleon forces Urbana IX, the older Tucson-Melbourne force and the modified one TM99. When we combine the Urbana IX 3NF with CD Bonn 2000 the strength of the repulsive part of this 3NF has been reduced by multiplying it with the factor 0.812 in order to get the proper E_{3H} .

Due to their nonnegligible influence on the nd scattering lengths, we took special care of electromagnetic interactions. In the case of the AV18 potential it is clear how to separate the strong AV18 force from the electromagnetic parts because both are well defined and added together in fitting the total force to the NN data. In case of the np system the EMI's are given in Eqs. (11), (12), and (15) of Ref. [14] and in Eq. (16) for the nn system (for the np system

we did not include the very small class IV charge asymmetric force $\propto \vec{L} \cdot 1/2(\vec{\sigma}_i - \vec{\sigma}_j)$. Also we neglected the energy dependence of the α' . This is different for the CD Bonn 2000 and Nijmegen potentials, which were fitted directly to the NN data without adding to them electromagnetic interactions, with the exception of the point Coulomb force in case of the pp system. Therefore to define the strong forces in the particular NN system one needs to subtract the corresponding EMI, which we assumed to be given as in ref. [14]. To be precise for the np system we subtract from the np CD Bonn and the Nijmegen forces the np EMI's as defined above. Similarly for the nn system we subtract from CD Bonn the MMI as defined above. Since we also want to see the effect of replacing the strong nn force by the strong pp force we have also to define the strong pp CD Bonn and Nijmegen forces. In this case we subtract from those potentials the pp EMI's as given in Eqs. (3)-(8) of Ref. [14] without the leading 1 in $F_c(r)$ from Eq. (10) of Ref. [14], since the point Coulomb force has been taken into account for those potentials fitting to the pp data.

Before we report on our results we give some comments on our numerical accuracy. As usual the partial wave decomposition is truncated at a certain total two-body angular momentum j_{max} . Fig. 1 documents the convergence of ${}^2a_{nd}$ as function of j_{max} . This shows that we reached an accuracy of about three digits. This is for CD Bonn [31] alone and valid also for the other NN forces alone. Adding a three-nucleon force we were limited to $j_{max} = 5$ due to computer resources. Nevertheless, as Fig. 2 documents, the convergence reached for ${}^2a_{nd}$ is two digits. In case of ${}^4a_{nd}$ with NN forces alone we reach 4 digits convergence and including a 3N force an accuracy close to that. This is documented in Fig. 3. The other numerical ingredients (discretization in the momenta) are safely under control. In all calculations we took into account charge dependence of the NN forces using a simple " $\frac{2}{3}t_{pp(nn)} + \frac{1}{3}t_{np}$ " rule to generate t-matrices in isospin $t = 1$ 2N states [32]. The total isospin $T = 3/2$ 3N states have been neglected [32]. We checked that their inclusion does not change ${}^4a_{nd}$ up to the fifth digit and the change of ${}^2a_{nd}$ is of the order of 0.1%. The triton binding energies have been obtained using $j_{max} = 6$. They are accurate to 2 keV.

As an overview we show all our results for ${}^2a_{nd}$ and E_{3H} in Fig. 4. We see a group of results in the right half of the figure based on NN forces alone and another group close to the experimental area including 3N forces. We performed several investigations. First we take CD Bonn 2000 as it is (fitted to the NN data) and use the np-nn force combinations appropriate to the nd system. In this way the EMI's in the np and nn systems are effectively included inside the strong forces. In case of AV18 we keep all electromagnetic corrections as in [14] except the energy dependence of α' (MMI's for the nn system and the MMI's together with the one photon Coulomb term $V_{C_1}(np)$ for the np system). The corresponding two predictions are shown as stars in Fig. 4.

Secondly we want to see the effect of replacing the strong nn forces by the strong pp forces. The difference between nn and pp strong forces is mostly located in the different scattering lengths a_{nn} and a_{pp} (strong) and will therefore give some information how changes in a_{nn} will show up in changes of ${}^2a_{nd}$. Since thereby we do not want to change the EMI's we keep in case of AV18 the nn MMI. For the CD Bonn and the Nijmegen potentials the strong pp potentials are defined as above and the nn MMI (as for AV18) is added. The results are shown as the 5 open circles in Fig 4. As seen in case of CD Bonn 2000 and AV18 the 3H binding energy is decreased and a_{nd} increased. For the Nijmegen potentials such a comparison is not done, since no nn forces have been introduced. The effects on the 3N

binding energies are known. These two first investigations provide theoretical predictions for the nd scattering lengths and triton binding energy including all electromagnetic interactions similarly as is the case for the measured values.

In the next two investigations we address the effects of the electromagnetic interactions themselves by switching them off while generating theoretical predictions. For the AV18 potential we take just the np-nn and np-pp strong force combinations alone, while in the cases of CD Bonn 2000, Nijm I, II, and 93 we only use the corresponding strong forces stripped off from the EMI's, as described above. The resulting theoretical predictions are shown as pluses and squares in Fig. 4 for the np-nn and np-pp combinations, respectively. Again the binding energy is decreased and a_{nd} increased.

The individual results of these four investigations are summarized in Fig. 4 also as dashed (np-nn with EMI's), dotted (np-pp with EMI's), solid (np-nn), and dashed-dotted (np-pp) straight lines fitted in a χ^2 sense. These lines include also the corresponding results including 3NF's (see below). We see a small shift of the lines under exchanges of nn versus pp forces, but a more significant shift if the electromagnetic forces are switched off. Though the two curves (dashed and dotted) for the cases when the electromagnetic forces are added come close to the experimental range spanned by the uncertainty in ${}^2a_{nd}$, they miss it clearly. When the electromagnetic forces are switched off the np-nn (solid) and np-pp (dashed-dotted) lines go through the experimental point well inside the ${}^2a_{nd}$ error bar.

Now we want to regard our results in more detail as displayed in Table I and in the inset of Fig. 4. The theory has to be finally compared to the experimental values, which are ${}^2a_{nd} = (0.65 \pm 0.04)$ fm [33], ${}^4a_{nd} = (6.35 \pm 0.02)$ fm [33], and $b_{nd} = (6.669 \pm 0.003)$ fm [21].

The results in Table I are grouped into NN force predictions only and selected combinations with the 3N forces TM, TM99 and Urbana IX. For each potential or potential combination we show the results for the various scattering lengths and the ${}^3\text{H}$ binding energies. This is given for the np-pp NN forces, with (without) EMI's in the first (second) row. For AV18 and CD Bonn 2000 we also show the results for np-nn forces with (third row) and without (fourth row) electromagnetic interactions. Note that in case of the np-nn forces including EMI's (as described above) the combinations with TM99 and Urbana IX are fitted well to the experimental value -8.48 MeV of the ${}^3\text{H}$ binding energy. This is also the case for Nijm I and II, which, however, refers to the np-pp forces. For the older TM 3N force we did not perform a precise (re)fit and the results are only included in view of investigating, whether a straight line correlation between ${}^2a_{nd}$ and E_{3H} exists. A glance at Fig. 4 tells that the individual results scatter around the four straight lines. Thus obviously no straight line correlation exist (this has been known before, though for some older calculations the numerical accuracy might be not sufficient to give a reliable judgement).

Let us now concentrate on the group of results with 3N forces. These are displayed in the inset of Fig. 4. We see four results (stars) for the np-nn forces including TM99 or Urbana IX, where the binding energy has been exactly fitted but where the ${}^2a_{nd}$ value is too small. These are the results achieved under the supposedly most realistic assumptions in this paper. If one switches off the electromagnetic interaction (pluses) the binding energy increases and interestingly ${}^2a_{nd}$ moves to larger values. Regarding all results, the inclusion of the electromagnetic force in our studies shows that they cause shifts of up to about 40 keV less binding energy and of up to about 0.04 fm decrease in ${}^2a_{nd}$. In no case studied the experimental value of ${}^2a_{nd}$ is reproduced for np-nn and np-pp strong forces combined

with different 3NF's with exception of np-pp AV18 combined with TM 3NF, for which the theoretical prediction lies at the lower limit of the error bar.

As one learned from the approach in chiral perturbation theory [13], where two parameters are needed to fix the short range 3N forces at NNLO and consequently two 3N observables to adjust them, one could foresee that the straight lines in Fig. 4 could only by accident pass through the experimental region. For the conventional forces used in this paper, one can think of additional 3N force diagrams (the most obvious one the $\pi - \rho$ exchange) where a sufficient number of parameters would be available to fit both, E_{3H} and ${}^2a_{nd}$.

Going back to Table I we see that ${}^4a_{nd}$ sticks always close to the value 6.34 for the np-pp and np-nn NN force choices, without or with 3N forces and with EMI's included. This is well within the experimental ${}^4a_{nd}$ error bar. Interestingly, the electromagnetic interactions increase ${}^4a_{nd}$ in nearly all cases by about 0.02 and the pure strong force predictions lie always outside the experimental error bar.

Finally, one can confront theory to the very precisely known experimental value of the coherent scattering length b_{nd} [21]. Clearly the supposedly most realistic dynamics (nn-pp NN forces plus TM99 or Urbana IX 3NF's) misses that value. As can be seen from Table I, when electromagnetic interactions are included the np-pp force combination reaches the experimental value in case of the AV18 and CD Bonn 2000 potentials combined with Urbana IX and AV18 with TM99. However, this agreement is accidental and caused by the corresponding decrease in 3H binding.

IV. SUMMARY AND OUTLOOK

A recently performed precise neutron interferometric measurement of the nd coherent neutron scattering length [21] and a planned precision measurement of the doublet nd scattering length [34] stimulated us to investigate the theoretical predictions of that quantity for the high precision NN forces CD Bonn 2000, AV18, Nijm I, II and 93 in combination with currently popular 3N force models. These are the modified 2π -exchange Tucson-Melbourne (TM99) and the Urbana IX 3N forces. We have chosen several NN and 3NF combinations, which are separately adjusted to the 3H binding energy. For NN forces alone with and without EMI's we recovered the approximate correlation between E_{3H} and ${}^2a_{nd}$, but the scatter around a thought straight line (Phillips line) inside the band spanned by the 4 lines in Fig. 4 is quite strong. Adding 3N forces shifts the values into the neighbourhood of the experimental range of ${}^2a_{nd}$, but misses the experimental value including its error bar in all cases, when electromagnetic forces are included. The inset of Fig. 4 clearly shows that for equal or nearly equal 3H binding energies ${}^2a_{nd}$ can vary significantly and vice versa.

Thus one has to conclude that ${}^2a_{nd}$ has to be considered as a low energy observable, which is independent from the 3H binding energy. This observation has been found before in approaches based on pure effective field theory (pionless formulation) and on chiral perturbation theory (including pion degrees of freedom). Thus in future investigations, adjusting both observables, E_{3H} and ${}^2a_{nd}$, for conventional nuclear forces will require more flexibility in the choice of 3N forces. Adding more mechanisms (on top of the 2π -exchange) for 3N forces should be no obstacle. This is a step already performed in the effective theory approaches [8–10,13].

We also investigated the effects on ${}^2a_{nd}$ resulting from electromagnetic interactions given in [14]. The effects on ${}^2a_{nd}$ and even ${}^4a_{nd}$ are noticeable. For ${}^2a_{nd}$ including the electromagnetic interactions reduces its value by up to 0.04 fm. It is interesting to note that ${}^4a_{nd}$ is perfectly stable under all exchanges of nuclear forces studied in this paper but the electromagnetic interactions affect its value, though only in the 3'rd digit. However, only when EMI's are included the experimental value is reproduced.

The effects of adding the electromagnetic interactions on the 3H binding energy are well known and can reach shifts of up to 40 keV less binding energy.

Due to the failure to describe ${}^2a_{nd}$ also the recently newly measured coherent scattering length b_{nd} cannot be reproduced theoretically. The good reproduction of ${}^4a_{nd}$ by all interactions and the small error bar of the coherent scattering length suggests that the value of the doublet nd scattering length might be somewhat smaller than the presently one, namely around 0.63 fm, different from the present experimental value of ${}^2a_{nd}$. This strongly calls for a new, more precise measurement.

Since the scattering lengths are (extreme) low energy observables, it appears that the mentioned effective theory approaches are the most adequate ones. Because one works there below a certain momentum cut off, which is smaller than the nucleon mass, they allow also to incorporate relativistic effects in a well defined and converged manner. Also 3N forces appear in those approaches in a well organised manner, according to a certain power counting scheme, and are consistent to the NN forces. In other words, one can take into account all these subtle effects, relativity, 3N forces, isospin breaking, in a well controlled and systematic manner. In conventional approaches on the other hand, which include a lot of phenomenological parametrisations and where no momentum cut-off is used, a reliable treatment of relativistic effects poses still a problem and the choices of 3N force mechanisms are also quite open. Therefore in conventional approaches physically reliable predictions to ${}^2a_{nd}$ will very likely remain a challenge for quite some time.

V. APPENDIX

This appendix summarizes various expressions exactly at the nd threshold $q_0 = 0$. The first part of the driving term in Eq.(1) turns out to be

$$\begin{aligned} \langle pq\alpha|tP|\phi \rangle &= \delta_{\lambda_0,0} \sum_{l_\alpha l_0 I_0} \langle pl_\alpha|t^\alpha(-\frac{3}{4m}q^2)|\frac{q}{2}l_{\alpha'} \rangle \varphi_{\alpha_0}(q) \\ &\quad (1m_d I_0 m_n |JM) (\lambda_0 0 \frac{1}{2} m_n |I_0 m_n) \sqrt{\frac{\hat{\lambda}_0}{4\pi}}. \end{aligned} \quad (9)$$

The quantities with index 0 refer to the initial state.

The kernel applied on T is given as

$$\begin{aligned} \langle pq\alpha|tG_0PT = \int q''^2 dq'' \\ \int_{-1}^{+1} dx \frac{\sum_{l_{\alpha'}} \frac{m}{qq''} \frac{t^{l_{\alpha'} l_{\alpha'}}(p, \pi_1; -\frac{3}{4m}q^2)}{\pi_1^{l_{\alpha'}}} \sum_{\alpha''} \frac{G_{\bar{\alpha}\alpha''}(q, q'', x)}{\pi_2^{l_{\alpha''}}} \langle \pi_2 q'' \alpha'' | T \end{aligned} \quad (10)$$

with

$$x_0 \equiv \frac{-k_d^2 - q'^2 - q^2}{qq''} \quad (11)$$

and $\bar{\alpha}$ contains the same quantum numbers as α with the exception of l_α replaced by $l_{\alpha'}$.

For our notation see [28]. The deuteron binding energy is written as $(-k_d^2/m)$. The remaining parts related to $V_4^{(1)}$ can be worked out correspondingly and can be found in [35]. Evaluating the elastic scattering amplitude one needs it at $q = q_0$ (see Eq.(4)). Therefore the point $q = q_0 = 0$ was included. Then Eq.(10) simplifies to

$$\begin{aligned} \langle pq = 0\alpha | tG_0PT = 2m\delta_{\lambda_\alpha,0} \int q''^2 dq'' \\ \sum_{l_{\alpha'}} \frac{t^{l_{\alpha'},l_{\alpha'}}(p, q''; 0) \sum_{\alpha''} 2^{l_{\alpha''}} g_{\bar{\alpha}\alpha''}^{0l_{\alpha'}0l_{\alpha''}0} \langle \frac{1}{2}q''q''\alpha'' | T}{-k_d^2 - q''^2}. \end{aligned} \quad (12)$$

One ends up with the elastic scattering amplitude at threshold:

$$\begin{aligned} U_{\lambda'I',\lambda I}^{J\pi} = & -\frac{2k_d^2}{m} \delta_{\lambda,0} \delta_{\lambda',0} g_{\alpha_d'\alpha_d}^{00000} \sum_{l,l'} \frac{\varphi_{l'}(p)}{p^{l'}} \Big|_{p=0} \frac{\varphi_l(p)}{p^l} \Big|_{p=0} \\ & + \delta_{\lambda',0} \sum_{l',\alpha''} 2^{l'+1} g_{\alpha_d'\alpha''}^{0l'0l''0} \int q''^2 dq'' \varphi_{l'}(q'') \langle \frac{1}{2}q''q''\alpha'' | T \\ & + \sum_{l'} \int p'^2 dp' \varphi_{l'}(p') \{V_4^{(1)}(1+P)\phi + V_4^{(1)}(1+P)G_0T\}_{\alpha_d',\lambda I}(p', 0). \end{aligned} \quad (13)$$

The geometrical coefficients $g_{\alpha\alpha'}^{kl_1l_2l'_1l'_2}$ arise from the permutation operator P and are given by Eq.(A19) in [28].

ACKNOWLEDGMENTS

This work was supported by the Deutsche Forschungsgemeinschaft (J.G.,R.S.), by the NFS grant No. PHY0070858, and by the NATO grant PST.CLG.978943. R.S. acknowledges financial support of the Foundation for Polish Science. The authors would like to thank Dr. E. Epelbaum for very constructive discussions. The numerical calculations have been performed on the Cray T90, SV1 and T3E of the NIC in Jülich, Germany.

REFERENCES

- [1] A.C. Phillips, Nucl.Phys. **A107**, 209 (1968); Rep. Prog. Phys. **40**, 905 (1977).
- [2] J.L. Friar, B.F. Gibson, G.L. Payne, Phys.Rev C **28**, 983 (1983).
- [3] J.L. Friar, B.F. Gibson, G.L. Payne, C.R. Chen, Phys. Rev. C **30**, 1121 (1984).
- [4] J.L. Friar, Few-Body Systems, Suppl **1**, 94 (1986).
- [5] C.R. Chen, G.L. Payne, J.L. Friar, B.F. Gibson, Phys. Rev. C **39**, 1261 (1989).
- [6] A. Kievsky, M. Viviani, S. Rosati, Nucl. Phys. A **577**, 511 (1994).
- [7] A. Kievsky, Nucl.Phys. A **624**, 125 (1997).
- [8] P.F. Bedaque, H.W. Hammer, U. van Kolck, Nucl. Phys. A **646**, 444 (1998).
- [9] P.F. Bedaque, U.van Kolck, Annu. Rev. Nucl. Part. Sci. **52**, 393 (2002).
- [10] P.F. Bedaque, G. Rupak, H.W. Griesshammer, H.W. Hammer, Nucl. Phys. A **714**, 589 (2003).
- [11] B. Blankleider, J. Gegelia, nucl-th/0009007.
- [12] B. Blankleider, J. Gegelia, Mesons & Light Nuclei '01, AIP Conf. Proc. **603**, 233 (2001).
- [13] E. Epelbaum, A. Nogga, W. Glöckle, H. Kamada, U.G Meissner, H. Witala, Phys.Rev. C **66**, 064001(2002).
- [14] R. B. Wiringa, V.G.J. Stoks, and R. Schiavilla, Phys. Rev. C **51**, 38 (1995).
- [15] R. Machleidt, Phys. Rev. C **63**, 024001 (2001).
- [16] V.G.J. Stoks, R.A.M. Klomp, C.P.F. Terheggen, J.J. de Swart, Phys. Rev. C **49**, 2950 (1994).
- [17] B. S. Pudliner, V. R. Pandharipande, J. Carlson, Steven C. Pieper, and R. B. Wiringa, Phys. Rev. C **56**, 1720 (1997).
- [18] J.L. Friar, D. Hüber, U. van Kolck, Phys. Rev. C **59**, 53 (1999).
- [19] S.A. Coon and H.K. Han, Few Body Systems, **30**, 131 (2001).
- [20] S.A. Coon *et al.*, Nucl. Phys. A **318**, 242 (1979); S.A. Coon, W. Glöckle, Phys. Rev. C **23**, 1970 (1981).
- [21] T.C. Black, private communication.
- [22] D.E. Gonzales Trotter *et al.*, Phys. Rev. Lett. **83**, 3788 (1999).
- [23] V. Huhn *et al.*, Phys. Rev. C **63**, 014003 (2000).
- [24] H. Kamada, W. Glöckle, J. Golak, Ch. Elster, Phys.Rev. C **66**, 044010 (2002).
- [25] A. Nogga, A. Kievsky, H. Kamada, W. Glöckle, L.E. Marcucci, S. Rosati, M. Viviani, Phys. Rev. C **67**, 034004 (2003).
- [26] W. Glöckle, H. Witala, D. Hüber, H. Kamada and J. Golak, Phys. Rep. **274**, 107 (1996).
- [27] D. Hüber, H. Kamada, H. Witala, and W. Glöckle, Acta Physica Polonica B **28**, 1677 (1997).
- [28] W. Glöckle, *The Quantum Mechanical Few-Body Problem*, Springer-Verlag, Berlin, 1983.
- [29] H. Witala, Th. Cornelius, and W. Glöckle, Few Body Systems, **3**, 123 (1988).
- [30] D. Hüber, W. Glöckle, J. Golak, H. Witala, H. Kamada, A. Kievsky, S. Rosati, and M. Viviani, Phys. Rev. C **51**, 1100 (1995).
- [31] R. Machleidt, F. Sammarruca, and Y. Song, Phys. Rev. C **53**, R1483 (1996).
- [32] H. Witala, W.Glöckle, H.Kamada, Phys. Rev. C **43**, 1619 (1991).
- [33] W. Dilg, L. Koester, and W. Nistler, Phys. Lett. **36B**, 208 (1971).
- [34] O. Zimmer, private communication.
- [35] D. Hüber, H.Witala, and W.Glöckle, Few Body Systems B **14**, 171 (1993).

TABLES

TABLE I. Doublet and quartet nd scattering lengths 2a and 4a together with the coherent scattering length b_{nd} for different NN potentials and selected combinations with different 3NF's. All calculations have been done with $j_{max} = 5$. The first and second rows give for each potential or potential combination the values obtained with np-pp strong potentials with and without EM interactions, respectively (see text for explanation). The third and fourth rows for AV18 and CD Bonn 2000 potentials and their combinations with 3NF's are the corresponding results when the pp strong NN potential is replaced by the nn one (keeping the nn MMI in case that EMI are included). The last column shows our 3H binding energies. We also included in the second column the cut-off parameter Λ for the TM and TM99 forces.

Potential	Λ/m_π	2a (fm)	4a (fm)	b_{nd} (fm)	E_{3H} (MeV)
CD Bonn 2000		0.976	6.347	6.837	-7.946
		1.011	6.324	6.833	-7.989
		0.925	6.347	6.812	-8.005
		0.943	6.324	6.798	-8.048
CD Bonn 2000+TM	4.795	0.622	6.347	6.661	-8.419
	4.795	0.661	6.324	6.657	-8.463
	4.795	0.570	6.347	6.634	-8.482
	4.795	0.590	6.324	6.622	-8.528
CD Bonn 2000+TM99	4.469	0.620	6.347	6.660	-8.422
	4.469	0.658	6.324	6.656	-8.466
	4.469	0.569	6.347	6.634	-8.482
	4.469	0.589	6.324	6.622	-8.527
CD Bonn 2000+Urb		0.637	6.347	6.668	-8.423
		0.674	6.324	6.664	-8.467
		0.586	6.347	6.643	-8.482
		0.607	6.325	6.630	-8.526
AV18		1.304	6.346	7.001	-7.569
		1.319	6.326	6.988	-7.606
		1.248	6.346	6.973	-7.628
		1.263	6.326	6.960	-7.666
AV18+TM	5.215	0.614	6.346	6.656	-8.478
	5.215	0.633	6.326	6.645	-8.518
	5.215	0.556	6.346	6.627	-8.545
	5.215	0.575	6.326	6.616	-8.584
AV18+TM99	4.764	0.645	6.346	6.671	-8.417
	4.764	0.663	6.326	6.660	-8.457
	4.764	0.587	6.346	6.643	-8.482
	4.764	0.606	6.326	6.632	-8.522
AV18+UrbIX		0.636	6.347	6.667	-8.418
		0.654	6.326	6.656	-8.458
		0.578	6.347	6.638	-8.484

		0.597	6.326	6.628	-8.523
Nijm I		1.158	6.342	6.924	-7.742
		1.190	6.321	6.919	-7.782
Nijm I+TM	5.120	0.601	6.342	6.646	-8.493
	5.120	0.638	6.321	6.643	-8.535
Nijm I+TM99	4.690	0.594	6.342	6.642	-8.485
	4.690	0.629	6.321	6.638	-8.528
Nijm II		1.231	6.345	6.964	-7.663
		1.259	6.325	6.957	-7.700
Nijm II+TM	5.072	0.598	6.345	6.647	-8.500
	5.072	0.630	6.325	6.643	-8.540
Nijm II+TM99	4.704	0.597	6.345	6.646	-8.487
	4.704	0.627	6.325	6.642	-8.527
Nijm 93		1.196	6.343	6.944	-7.672
		1.225	6.322	6.937	-7.712
Nijm 93+TM	5.212	0.574	6.343	6.633	-8.502
	5.212	0.608	6.322	6.629	-8.543

FIGURES

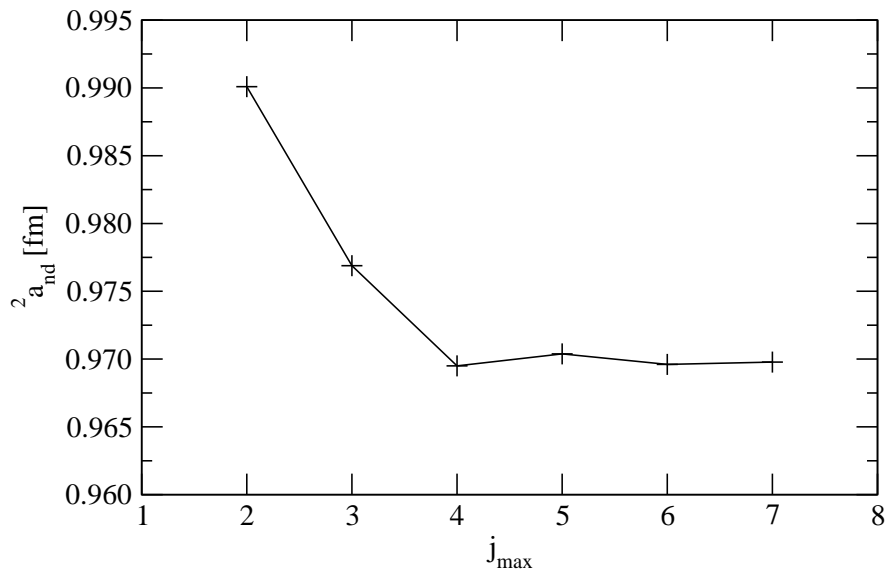


FIG. 1. The convergence of the doublet scattering length ${}^2a_{nd}$ as a function of the 2N total angular momentum j_{max} for the CD Bonn potential.

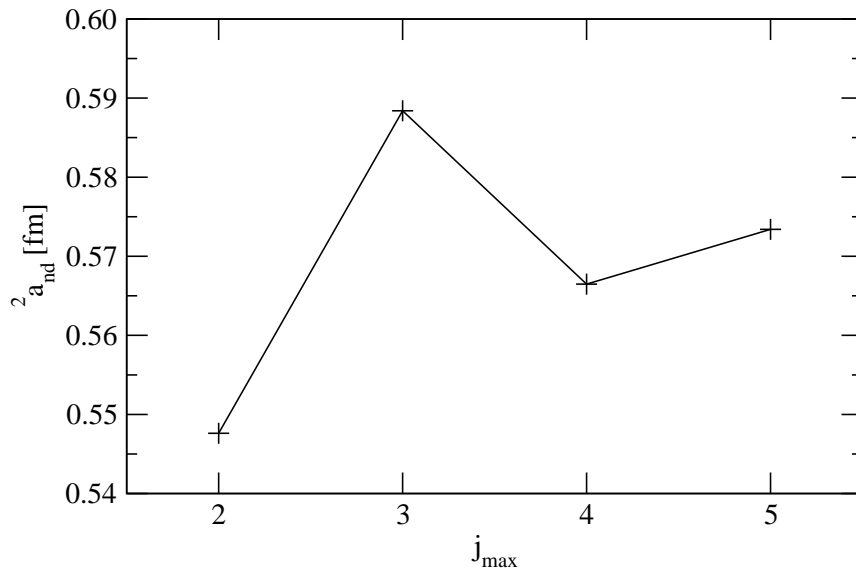


FIG. 2. The same as in Fig. 1 for the CD Bonn potential combined with the TM 3NF.

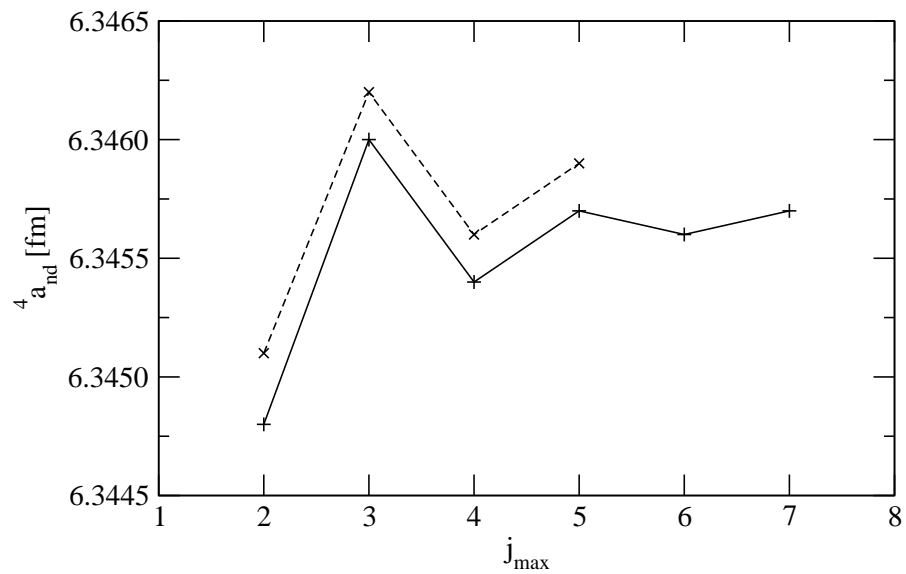


FIG. 3. The convergence of the quartet scattering length ${}^4a_{nd}$ as a function of j_{\max} for the CD Bonn potential (solid curve) and its combination with the TM 3NF (dashed curve).

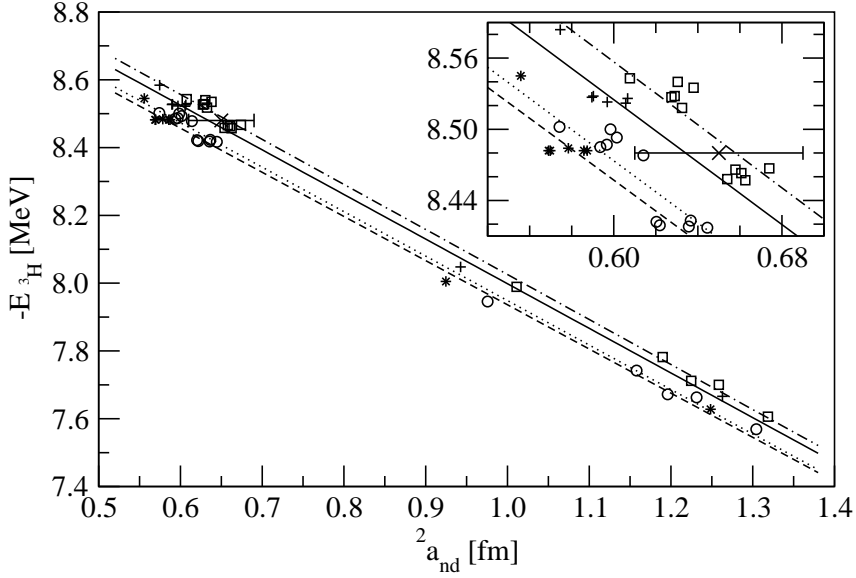


FIG. 4. The results for ${}^2a_{nd}$ and E_{3H} from Table I: np-nn forces alone (pluses), np-pp forces alone (squares), and np-nn and np-pp forces plus electromagnetic interactions (stars and circles, respectively). The four straight lines (Phillips lines) are χ^2 -fits (np-nn: solid, np-pp: dashed-dotted, np-nn with EMI's: dashed, np-pp with EMI's: dotted). The lines with EMI's miss the experimental error bar for ${}^2a_{nd}$ [33]. The physically interesting domain around the experimental values is shown in the inset.